Biochemistry and Biophysics Reports 27 (2021) 101037

Contents lists available at ScienceDirect

Biochemistry and Biophysics Reports

journal homepage: www.elsevier.com/locate/bbrep

Cardiac phospholipidome is altered during ischemia and reperfusion in an ex vivo rat model

Javier-Fernando Montero-Bullon [a,1], Susana S. Aveiro [a,1], Tânia Melo [a,b], Tânia Martins-Marques [c,d], Diana Lopes [a,b], Bruna Neves [a], Henrique Girão [c,d], M. Rosário M Domingues [a,b], Pedro Domingues [a,*]

[a] Mass Spectrometry Centre, LAQV REQUIMTE, Department of Chemistry, University of Aveiro, Santiago University Campus, 3810-193, Aveiro, Portugal
[b] CESAM, Centre for Environmental and Marine Studies, Department of Chemistry, University of Aveiro, Santiago University Campus, 3810-193, Aveiro, Portugal
[c] Coimbra Institute for Clinical and Biomedical Research (iCBR), Faculty of Medicine, University of Coimbra, Coimbra, Portugal
[d] CNC.IBILI, University of Coimbra, Coimbra, Portugal

ARTICLE INFO

Keywords:
Lipidomics
Acute myocardial ischemia/reperfusion injury: heart attack
Ischemia
Reperfusion
Phospholipidome
Liquid chromatography
Mass spectrometry

ABSTRACT

Acute myocardial infarction (AMI) is the leading cause of death, morbidity, and health costs worldwide. In AMI, a sudden blockage of blood flow causes myocardial ischemia and cell death. Reperfusion after ischemia has paradoxical effects and may exacerbate the myocardial injury, a process known as ischemic reperfusion injury. In this work we evaluated the lipidome of isolated rat hearts, maintained in controlled perfusion (CT), undergoing global ischemia (ISC) or ischemia followed by reperfusion (IR). 153 polar lipid levels were significantly different between conditions. 48 features had $q < 0.001$ and included 8 phosphatidylcholines and 4 lysophospholipids, which were lower in ISC compared to CT, and even lower in the IR group, suggesting that IR induces more profound changes than ISC. We observed that the levels of 16 alkyl acyl phospholipids were significantly altered during ISC and IR. Overall, these data indicate that myocardial lipid remodelling and possibly damage occurs to a greater extent during reperfusion. The adaptation of cardiac lipidome during ISC and IR described is consistent with the presence of oxidative damage and may reflect the impact of AMI on the lipidome at the cellular level and provide new insights into the role of lipids in the pathophysiology of acute myocardial ischemia/reperfusion injury.

1. Introduction

Acute myocardial infarction (AMI) is one of the major cardiovascular diseases (CVD) that results in higher mortality and morbidity rates in developed and underdeveloped countries. According to the World Health Organization, AMI contributes around 10% of total global mortality [1]. AMI is characterised by damage to myocardial tissue and cell death resulting from sudden deficiency of blood flow, and therefore lack of nutrients and oxygen in a region of the heart [2,3]. AMI lesions are the result of a multifactorial pathological process, including oxidative stress and increased production of reactive oxygen species (ROS), as well as mitochondrial dysfunction, which ultimately leads to the death of cardiomyocytes [4,5]. Increased production of ROS can alter redox homeostasis, causing not only the oxidation of lipids and proteins but also the activation of several signalling pathways and inflammation [6,7]. This pro-inflammatory response in AMI contributes to cell dysfunction, cardiomyocyte death and myocardial injury [8]. The outcome and recovery of AMI depend largely on the magnitude of the ischemic event and the activation of the cellular response by cytoprotective mechanisms [9,10], such as autophagy [11–14], as well as the rapid restoration of blood flow.

The response to myocardial ischemia-reperfusion (IR) may have paradoxical effects. It is necessary to restore nutrient and oxygen supply, and reperfusion can exacerbate cell damage in a process known as IR injury [15], which has been associated with a burst of oxidative stress and inflammation [3,16,17]. Although ROS have been consistently associated with IR injury, the mechanisms and signals involved in this damaging process remain largely elusive. This lack of knowledge aggravates the definition of AMI outcomes, diagnostic and prognostic factors, hindering progress in health care [18–20].

* Corresponding author. Department of Chemistry, University of Aveiro, Campus Universitário Santiago, 3810-193, Aveiro, Portugal.
E-mail address: p.domingues@ua.pt (P. Domingues).
[1] Both authors contributed equally to this manuscript.

https://doi.org/10.1016/j.bbrep.2021.101037
Received 23 February 2021; Received in revised form 25 May 2021; Accepted 25 May 2021
Available online 10 June 2021

Lipids are involved in CVD and AMI, not only as ROS targets but also due to the adaptation of lipid metabolism in these processes. Lipidomic analysis performed in plasma revealed an increase in free fatty acid levels at the onset of AMI [21,22] and in oxidised low-density lipoprotein [23]. Omega-3 and stearic acids were inversely correlated with the risk of AMI, while arachidonic acid and oxylipins were positively correlated [24]. Changes in phospholipids and sphingolipids have also been reported in AMI [25,26] and correlated with CVD incidence [27], mortality [28] or prognosis [29]. The change in phosphatidylcholine levels was correlated with the risk of CVD [30], while a decrease in plasmalogens levels has also been observed in the plasma of patients with AMI [31] and has been reported in cardiac remodelling and restoration of cardiac function [32].

Lipid changes associated with AMI and IR in cardiac tissue of animal models or cells included changes in the profile of glycerolipids, sphingolipids, and free fatty acids [33], as well as depletion of cardiolipins (CLs) [34]. Also, the sphingolipid profile has been shown to vary in blood samples from rats with AMI [35–38] and infarcted heart [37]. Recently, it has also been shown that the phospholipid profile of myoblast cells, namely phosphatidylcholines (PC), lysophosphatidylcholines (LPC), phosphatidylethanolamines (PE), phosphatidylserines (PS), phosphatidylinositol (PI), cardiolipins (CL) and sphingomyelins (SM) classes, changes in ischemia [39]. However, to date, no study has addressed the profile of phospholipids associated with ischemia (ISC) and subsequent reperfusion (IR) in heart tissue.

In this study, we compared the lipidome of cardiac tissue, in isolated control rat hearts (CT), myocardial ischemia (ISC) and ischemia-reperfusion (IR), to determine whether the ISC and the IR would induce distinct changes in the cardiac tissue lipidome. High-resolution hydrophilic interaction liquid chromatography-mass spectrometry (HILIC LC-MS) was used for lipidomic profiling of cardiac tissue from animal models using the ex vivo Langendorff apparatus, widely used by the scientific community for cardiovascular research, particularly for unbiased and non-targeted omics approaches [40].

2. Materials and methods

2.1. Chemicals

Phospholipids internal standards for LC-MS were 1,3-bis [1,2-dimyristoyl-*sn*-glycero-3-phospho]-*sn*-glycerol) (CL (14:0)$_4$), 1,2-dimyristoyl-*sn*-glycero-3-phosphocholine (dMPC), 1-nonadecanoyl-2-hydroxy-*sn*-glycero-3-phosphocholine (LPC(19:0)), 1,2-dimyristoyl-*sn*-glycero-3-phosphoethanolamine (dMPE), 1,2-dimyristoyl-*sn*-glycero-3-phosphate (dMPA), 1,2-dimyristoyl-*sn*-glycero-3-phospho-(10-rac-glycerol) (dMPG), 1,2-dimyristoyl-*sn*-glycero-3-phospho-L-serine (dMPS), 1,2-dipalmitoyl-*sn*-glycero-3-phospho-(1′-myo-inositol) (dPPI) and N-heptadecanoyl-D-*erythro*-sphingosylphosphorylcholine (SM(17:0/d18:1)), purchased from Avanti polar lipids Inc. (Alabaster, AL) as 99% pure chloroform stock solutions and used without further purification.

2.2. Ex vivo langendorff heart perfusion model

Animals were obtained from our local breeding colony and handled according to the European Union (EU) guidelines (2010/63/EU) and to the Portuguese law of animal welfare (DL 129/92, DL 197/96; P 1131/97), with approval of the Ethics Committee, Faculty of Medicine, University of Coimbra (ORBEA-IBILI, permit 13/2015). 10-week-old female Wistar rats (400 ± 25 g) were anaesthetized with 85 mg/kg ketamine and 10 mg/kg xylazine and heparinized, after which hearts were excised and perfused on a Langendorff apparatus. Modified Krebs–Henseleit (KH) buffer (118 mM NaCl, 25 mM $NaHCO_3$, 4.7 mM KCl, 1.2 mM $MgSO_4$, 1.2 mM KH_2PO_4, 10 mM Hepes, 1.25 mM $CaCl_2$ and 10 mM glucose, pH 7.4) was used to perfuse the isolated hearts, at a constant flow rate of 15 ml/min, equilibrated with 95%O_2/5%CO_2 at 37 °C. After a 10 min stabilization period, hearts were either perfused for a further 20 min (CT; n = 3), subjected to 20 min of no-flow ischemia (ISC; n = 3), or 20 min of reperfusion after ischemia (IR; n = 3). After the experiments, hearts were snap-frozen in liquid nitrogen before subsequent analysis.

2.3. Tissue sampling and lipid extraction

Myocardial tissue (0.1 g) was excised from the hearts of the rats, and the tissue was transferred to a mortar and homogenized by adding liquid nitrogen and grounding with a pestle. The grounded tissue was collected in an ice-cold glass tube, and 1.5 mL MeOH was added, followed by liquid-liquid lipid extraction with methyl *tert*-butyl ether (MTBE) as previously described [41]. Briefly, MTBE was added to each sample and incubated for 1 h on ice with an orbital shaker. After centrifugation the upper organic phase containing the extracted lipids was collected. The lower phase was re-extracted, centrifuged and combined with the previous organic phase. After being dried under a nitrogen stream, the lipid extract was resuspended in $CHCl_3$ and used for the MS analysis and the quantitation of phospholipids. All analyses were performed on three biological replicates.

2.4. Quantification of phospholipids content by phosphorous assay

The total phospholipid content of samples was determined according to Bartlett and Lewis [42]. Briefly, an aliquot of 10 μL of the extract was dried and incubated for 1h at 180 °C with 125 μL of perchloric acid (70%). This solution and standards solutions were diluted (825 μL of water) and mixed with 125 μL of ammonium molybdate tetrahydrate (2.5% m/v) and 125 μL of ascorbic acid (10% m/v). Samples and standards were then simultaneously incubated at 100 °C and the content of inorganic acid was measured at 797 nm wavelength.

2.5. Fatty acids profiling by GC-MS

FAMEs (fatty acids methyl esters) were obtained by transesterification of total lipid extract. The lipid extracts (30 μg in $CHCl_3$) were dried under N_2 stream, redissolved in 1 mL of hexane, and mixed with 200 μL of a 2 M solution of KOH in methanol [43]. The reaction products were washed with 2 mL of saturated NaCl solution and the upper organic phase was dried and resuspended in 80 μL of hexane. Samples (4 μL) were injected in an Agilent Technologies 6890 N Network GC spectrometer (Santa Clara, CA) equipped with a polar DB-FFAP column of 30 m of length, 0.32 mm of internal diameter, and 0.25 μm film thickness (J&W Scientific, Folsom, CA). The GC equipment was connected to an Agilent 5973 Network Mass Selective Detector (Santa Clara, CA) scanning between *m/z* range 40–500 in a 1s cycle of full scan mode acquisition and electron impact adjusted at 70 eV of energy. The oven temperature was programmed with an initial temperature of 80 °C, following a linear increase to 160 °C at 25 °C/min, a linear increase to 210 °C at 2 °C/min, and finally linear increase until 250 °C at 30 °C/min, where it was held for 10 min before returning to the initial conditions. The injector and detector temperatures were 220 and 280 °C, respectively. Helium was used as carrier gas at a flow rate of 0.5 mL/min. A mixture of fatty acid methyl ester standards (Supelco 37 Component FAME Mix, CRM47885, Sigma Aldrich, St. Louis, MO, USA) was injected in the same session. Three technical replicates were used to confirm reproducibility.

2.6. Lipid profiling by HILIC-ESI-MS and MS/MS

An amount of lipid extract equivalent to 5 μg of total phospholipid was suspended in 200 μL of eluent B (60% ACN/40% MeOH (v/v), 1 mM ammonium acetate). The solution was spiked with 1 μL of a mixture of standards prepared by dissolving 25 μg of dMPC, 25 μg of dMPG, 25 μg of dMPE, 100 μg of dMPS, 50 μg of dPPI, 100 μg of dMPA, and 50 μg of LPC(19:0), 25 μg of SM(17:0/d18:1), 100 μg of CL (14:0)$_4$ to a final

volume of 1 mL of $CHCl_3$:MeOH (1:1). The preparation was transferred to a vial, and 5 μl were injected in a high-performance HPLC system with an autosampler (Accela™ Thermo Fisher Scientific, Waltham, MA, USA) coupled online to an Orbitrap Q-Exactive mass spectrometer (Thermo Fisher Scientific, Waltham, MA, USA). The chromatographic column was a microbore Ascentis Si HPLC Pore column (15 cm × 1.0 mm, 3 μm; Sigma–Aldrich). The solvent system consisted in a biphasic gradient with solvents A (50% acetonitrile/25% methanol/25%water (v/v/v), 1 mM ammonium acetate) and B (60% ACN/40% MeOH (v/v), 1 mM of ammonium acetate). The initial condition with 0% of mobile phase A held isocratically for 8 min, followed by a linear increase to 60% of A within 7 min and again held isocratically for 15 min, returning to the initial conditions in 5 min and equilibrating during 10 min. The flow rate was at 40 μL/min, and the column compartment was held at 30 °C. The Orbitrap Q-Exactive was operated simultaneously in positive mode (3 kV) and negative mode (−2.7 kV), with capillary temperature 250 °C, flow 15 U of sheath gas and 5 U of auxiliary gas (arbitrary units). The acquisition mode was data-dependent MS/MS, with MS at high resolution (resolution of 70,000, AGC target 10^6) and data-dependent MS [2] for the ten more intense peaks (resolution of 17,500, AGC target 10E [5], dynamic exclusion 30 s and threshold 10^4, and normalized collision energy ranged between 20, 30, and 35 eV). Data acquisition was carried out during the initial 35 min of the run using the Xcalibur data system (V3.3, Thermo Fisher Scientific, Waltham, MA, USA). At least three technical replicates were employed to confirm reproducibility.

2.7. Data analysis and statistics

All GC-MS chromatograms were analyzed using the MSD Cessation software version D.00.00.38 (Agilent Technologies, Santa Clara, CA, USA). The peaks were automatically integrated, the fatty acids were identified (mass spectrum and retention times), and the percentages of the total peak area were calculated.

LC-MS data were analyzed with Xcalibur Qual Browser (Thermo Fisher Scientific, Waltham, MA, USA) for chromatographic profiling, and high-accuracy MS and MS/MS identification of the phospholipid species. The species positively identified were quantified in MZMine 2.26 .[44] Data pre-processing, including baseline correction, peak deconvolution, deisotoping and alignment, and gap-filling, was applied. The identification of all lipid species was based on mass accuracy, retention time and manual analysis of MS/MS data. PE, LPE, PC, LPC, SM and Cer were analyzed in positive ion mode and identified as [M+H]+molecular ions, and PE, LPE, PA, PI, LPI, PS, PG and CL were identified in negative ion mode and identified as $[M - H]^-$ molecular ions and PC and LPC as $[M + CH_3COO]^-$ as adduct ions. Semi-quantification was performed by integrating the area under the curve using the negative mode LC-MS chromatographic peak of the ions for all lipid species except for PC, LPC, SM and Cer, where the positive mode data was used. Data (peak areas) were normalized by calculating the ratio against a selected internal standard.

Multivariate and univariate analyses were performed using R version 3.6.2 [45] in Rstudio version April 1, 1103 .[46] GC data were generalized log (glog) transformed and LC-MS data were glog transformed, EigenMS normalized [47], and autoscaled using the R package MetaboAnalystR [48]. Principal Component Analysis (PCA) was conducted for exploratory data analysis, with the R package pcaMethods [49]. Kruskal-Wallis test was used for nonparametric comparisons of median values among the three groups, followed by nonparametric pairwise multiple-comparison procedure using Dunn test. These tests were performed with the R built-in functions. P-values were corrected for multiple testing using the BH Benjamini, Hochberg, and Yekutieli method (q values) [50]. PCA and boxplot graphics were created using the R package ggplot2 [51]. Other R packages used for data management and graphics included plyr [52], dplyr [53], tidyr [54] and ggrepel [55].

3. Results

In our model of ischemia/reperfusion injury, electron microscopy data did not reveal major ultrastructural changes in ischemic hearts (no evidence of sarcolemmal or mitochondrial disruption, data not shown). Also, we observed a reduction in contractile cardiac function after 20 min of ischemia and the heart spontaneously beats upon reperfusion, demonstrating that viability and contraction function are preserved, even after 20 min of ischemia. These results are consistent with previous studies demonstrating that brief periods of ischemia do not induce significant cell death [56,57].

In this work, lipid extracts were obtained from rat hearts under three different conditions, namely maintained in control perfusion (CT), or subjected to ischemia (ISC), or ischemia and reperfusion (IR). These extracts were analyzed by two complementary analytical approaches: GC-MS, to study the profile of fatty acids (FA), and high-resolution HILIC LC-MS and MS/MS to study the profiles of polar lipids.

Using GC-MS analysis of the lipid extracts, we semi-quantified seven main fatty acids (FA) observed under the three conditions CT, ISC and IR. Under all conditions, stearic acid (C18:0) and linoleic acid (C18:2) were the most abundant FAs, followed by arachidonic acid (C20:4) and palmitic acid (C16:0), which is consistent with the FA profile reported in the literature for heart tissue [58]. As shown in Fig. 1, the main changes in relative abundance (RA) were an increase in the relative abundance of C18:0 in IR compared to CT ($p < 0.001$) and a decrease in ISC conditions compared to IR ($p < 0.05$) and the relative abundance of C18:0 fatty acid was IR ≥ ISC > CT); a decrease in the relative abundance of C18:2 in IR compared to ISC ($q < 0.01$) and the relative abundance of C18:2 was (IR < ISC ≈ CT); and a decrease in the relative abundance in IR compared to CT ($p < 0.05$) in C16:1 and C18:1, and the relative abundance was IR < CT ≈ ISC.

In our study, we chose to use alkaline transmethylation, which involves the use of a simple and rapid protocol. This approach also has the advantage of having good efficiency for fatty acids in phospholipids and it does not derivatize free fatty acids and fatty acids in cholesterol [59]. In this case, it is advantageous because its results can be directly compared with those of HPLC-MS. However, the higher sensitivity and selectivity of the LC-MS-based approach allows many more species to be identified than in the GC-MS approach. In addition, GC analysis of complex biological extracts may be inadequate in some situations, especially for relatively low abundance FAMEs [60].

In this study, we also assessed the cardiac lipid profile under the three experimental conditions (CT, ISC and IR) by high-resolution LC-MS and MS/MS analysis. We have identified and semi-quantified a total of 211 species of polar lipids divided into 11 classes: phosphatidylcholines (PC), lysophosphatidylcholines (LPC), phosphatidylethanolamines (PE), lysophosphatidylethanolamines (LPE), phosphatidylglycerols (PG), phosphatidylinositols (PI), lysophosphatidylinositol (LPI),

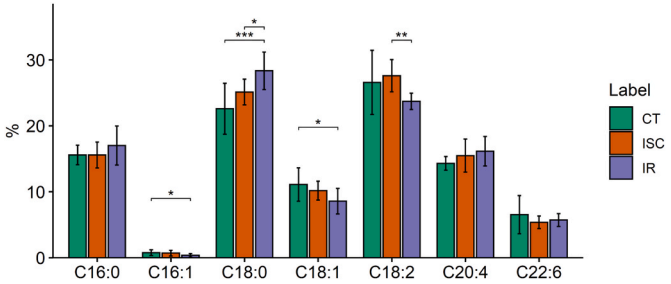

Fig. 1. Bar graph of the fatty acid profile obtained by GC-MS, for the three conditions: control (CT), ischemia (ISC) and ischemia-reperfusion (IR). Bars represent the percentage of each species of fatty acid in heart tissue. Data are presented as mean ± SD. Statistical tests were performed using the Kruskal-Wallis test followed by the Dunn multiple comparison test. ***$p < 0.001$, **$p < 0.01$, *$p < 0.05$.

phosphatidic acids (PA), phosphatidylserines (PS), cardiolipins (CLs), and sphingomyelins (SMs) (Supplementary Table S1). Seven lipid species of ceramides (Cer) have also been identified.

Preliminary principal component analysis (PCA) was then used for quality control and to investigate outliers and whether samples were pooled based on experimental conditions. PCA of the lipid profiles of the samples showed clustering of the three groups with a small overlap of the 95% confidence curve of the IR and ISC samples (Fig. 2). No outliers were observed. The explained variances were respectively 34.5% and 13.1% for the first and second components. Variables with contributions to the first principal component >1% included 14 PCs, 5 CLs, 2 PCs plasmalogen (PC–P), 1 PE, 1 LPE, 1 PE plasmalogen (PE-P), 1 PA and 1 SM (Supplementary Table S2).

Univariate analysis (Kruskal–Wallis followed by Dunn post-hoc analysis) was then used to test for significant differences in polar lipid species between the three conditions (CT, ISC and IR). The Kruskal-Wallis H test showed that 153 lipid levels were significantly different between conditions, of which 48 species had $q < 0.001$ (Supplementary Table S3). These 47 most important species of phospholipids included 17 species of PC, 5 PE, 8 PI, 4 lyso and 1 PA species. Dunn's multiple comparison test revealed that 128 species were significantly different between CT and IR, 80 between CT and ISC and 80 between IR and ISC, as detailed in Supplementary Table S4.

Fig. 3A shows the boxplots of the 12 phospholipid species with lower q-value and Fig. 3B shows the boxplots of the four lysophospholipids with $q < 0.001$. Of these species, all except the four lysophospholipids showed a lower abundance value in the IR samples. All phospholipids had a higher relative abundance value in controls showed a lower abundance value in the IR samples. All phospholipids had a higher relative abundance value in controls.

Our results also show that the levels of 16 alkyl acyl phospholipids (8 alkyl acyl PC, 8 alkyl acyl PE) were significantly altered during ISC and IR (Fig. 4).

4. Discussion

Deregulation of lipid metabolism is a hallmark of CVD, although it is not yet well understood. Although scarcely used, lipidomics is becoming a promising approach in the study of CVD [61,62]. In this work, we evaluated lipidome changes in an ex vivo model of ischemia (ISC) and ischemia-reperfusion (IR) in isolated Langendorff rat hearts. For this, we evaluated the fatty acid content by GC-MS and the phospholipid profile by LC-MS and MS/MS.

Data acquired by GC-MS showed an increase in the abundance of C18:0 fatty acid in IR, compared to CT (Fig. 1). The same trend, although not statistically significant, was observed in C16:0. Additionally, in the IR group, we observed a decrease in C16:1, C18:1, compared to CT and in the IR group we observed a decrease in C18:2, compared to ISC. The more pronounced effect observed in IR is consistent with the data reported in previous studies using cardiomyocytes [43] and human serum and heart tissue after AMI [24,58,63]. This decrease in polyunsaturated fatty acids (PUFAs) can occur due to fatty acid oxidation [64] because unsaturated fatty acyl chains are very sensitive to oxidation by ROS. Our data also show a tendency for, compared with the ISC group, the relative abundance of fatty acids in the IR group to be more different from those found in CT.

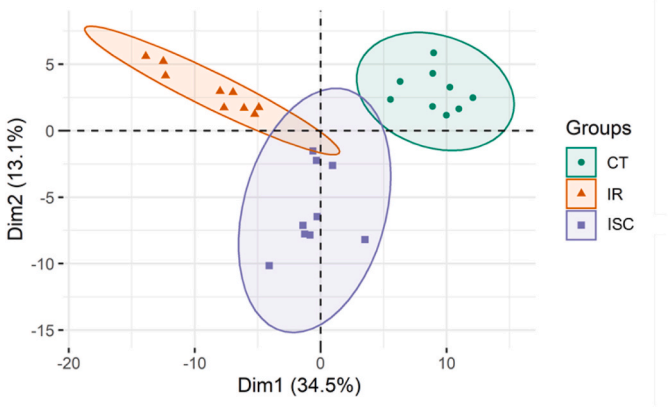

Fig. 2. PCA score plot of the first and third principal components of the PCA for the dataset on lipids acquired by LC-MS, of the three biological groups: control (CT), ischemia (ISC) and ischemia-reperfusion (IR).

Polar lipid data obtained using high-resolution LC-MS, from CT, ISC and IR tissue samples were initially analyzed by multivariate principal component analysis (PCA). The analysis of the PCA score plot (Fig. 1) showed that the features clustered the samples into the CT, ISC and IR groups. The main contributors to the first dimension included 14 PC species out of 26 with contributions above 1% (supplementary Table S2). Since PCs are the major component of cell membranes, these results suggest rapid constitutional changes at the membrane level during ISC and IR and that these changes could be indicative of these membrane modifications. Additionally, these phospholipids had a high number of double bonds, suggesting that the relative abundance of these species was more influenced by ISC and IR conditions. Taken together, these results strongly suggest that ISC, but mainly IR, induced changes in structural phospholipids in heart tissue.

Of the 211 lipid species identified in this study, 153 lipid levels were significantly different between conditions were statistically significant ($q < 0,05$), of which 48 species had $q < 0.001$ (Supplementary Table S3). These 48 most important lipids species included 17 PC species, showing that significant structural changes occur in cardiomyocytes during ISC and IR. Multiple pairwise comparisons (Supplementary Table S4) showed that most of these significant variations in relative lipid abundance occurred between CT versus IR (128 species), followed by CT versus ISC and IR versus ISC (80 species each). This suggests that reperfusion induced more profound changes than ISC, which is consistent with previous reports suggesting that the injury usually associated with ischemia is intensified during reperfusion [17,65–68].

Our results showed that four lysophospholipids with qvalues <0.001, LPC 18:0, LPE 16:0, LPC 20:3 and LPI 20:4, had lower abundances of ISC and IR, compared to the control (Fig. 3A). Previously, in a study of the rat heart following myocardial infarction the authors showed an increase of the levels of three LysoPC and one LysoPG, although no statistical analysis was shown [33]. ROS as well as lipid modifying enzymes, such as lipases and phospholipases, can produce lysophospholipids, and these molecules play a very important role in many cellular processes, such as cell adhesion, cell migration and cell survival, with messenger functions but also as inflammatory, and cytotoxic mediators (reviewed in [69]). For example, Phospholipase D1 (PLD1), a phosphatidylcholine (PC)-specific PL has been shown to be overexpressed in the infarcted myocardium in mice and after cardiac ischemia and reperfusion injury. This increase overexpression of PLD1 was linked to an increased in the size of the infarct size and to an impairment of left ventricular function [70]. These authors showed that PLD1 plays an important role in Tumor Necrosis Factor-alpha (TNF-α) mediated inflammation and scar formation after acute myocardial infarction in mice. A subsequent study identified PLD1 as a regulator of innate immunity and apoptosis [71]. In our study, although there were no significant changes between ISC and IR, there was a tendency for the levels of these lyso species to be lower in ISC than in IR, except for LPE16:0. Lysolipids bearing polyunsaturated fatty acyl chains such as LPC 22:6 and LPC 20:4 were associated with anti-inflammatory effects [72,73]. Therefore, the decrease observed in this study could be associated with a decrease in anti-inflammatory defences during ISC and IR.

Another feature of this study was the variation in the abundance of several PC species containing PUFAs. For example, the list of the 12 lowest qvalues PCs included 3 phosphatidylcholines with C34 (PC 34:3, PC 34:4, PC 34:5), 1 phosphatidylcholine with C36 (PC 36:5) and two

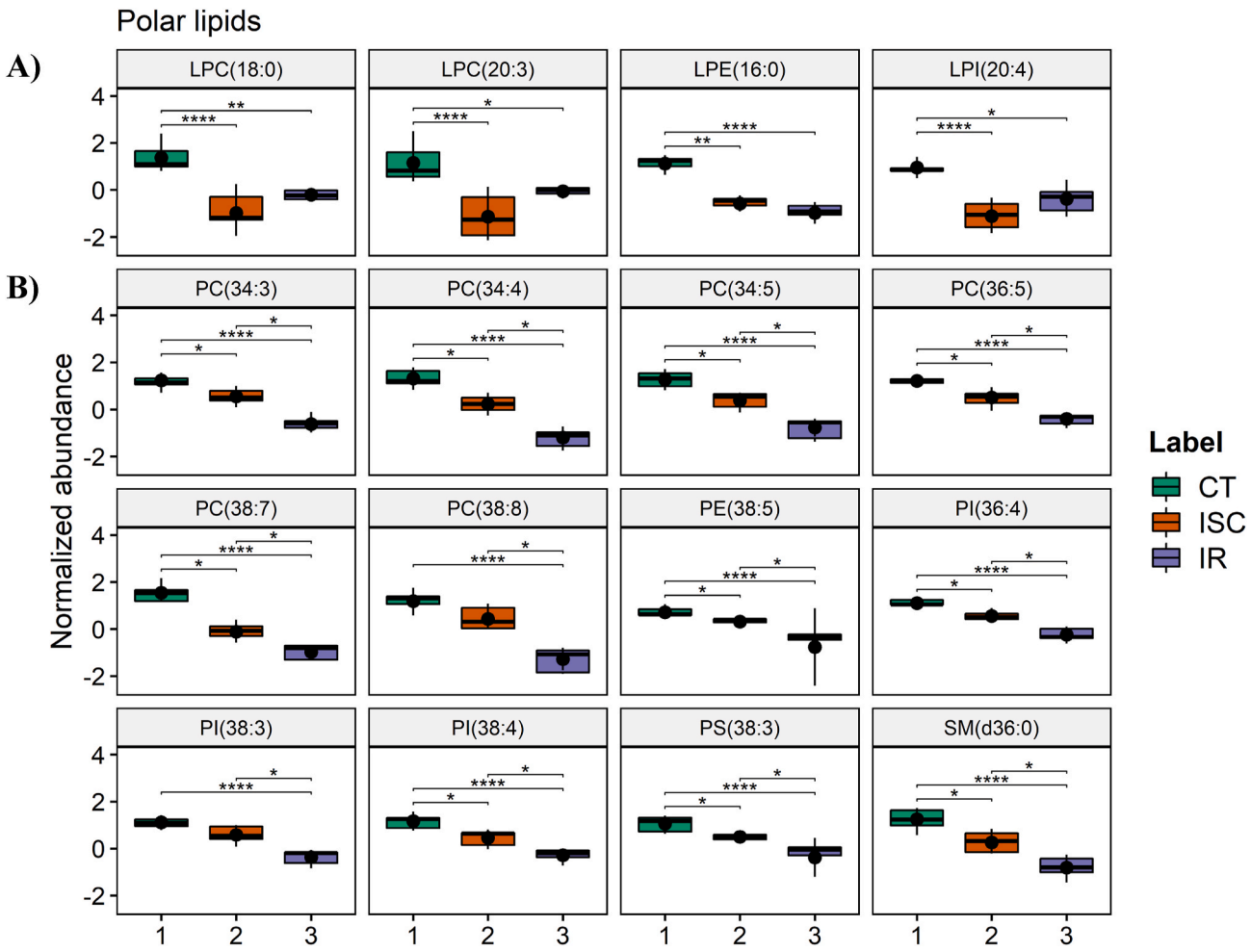

Fig. 3. Boxplots of a) the four lysophospholipids with q < 0.001; b) major 12 significantly different phospholipids species. Statistical tests were performed using the Kruskal-Wallis test followed by Dunn's multiple comparison test. Lipid species labels are in the following notation: PL (C:N) (PL = phospholipid class; C = total of carbon atoms in fatty acids; N = number of double bonds). Three groups were studied: 1-Control (CT), 2-ischemia (ISC) and 3-ischemia-reperfusion (IR) ****q < 0.001, ***q < 0.001, **q < 0.01, *q < 0.05.

with C38 (PC 38:7, PC 38:8) (Fig. 3B), all with a high degree of unsaturation. All these PCs had lower levels in IR and ISC, being the ordered levels CT > ISC > IR. These results are in agreement with the results observed in the GC-MS analysis of fatty acids, where the fatty acids C16:1, C18:1 and C18:2, tended to have lower abundance in IR. PCs containing PUFAs are prone to radical oxidation [74], and their oxidative degradation may justify the reduction observed during ISC and IR. In this case, our results show that the degradation by oxidation is maximal during reperfusion and not during ischemia. Although the effect of AMI on myocardial lipidome is scarcely discussed, a decrease in PCs has already been reported in IR [75,76]. Decreased PUFA levels in PC have been reported in other heart conditions, such as cardiomyopathy associated with diabetes [77]. Furthermore, an increase in lipid peroxidation [78] and the presence of molecular species of oxidised PC have been reported following myocardial ischemia and associated with cell death of cardiomyocytes [79]. This increase in lipid peroxidation was also demonstrated by the presence of oxidised PC species, such as 1-palmitoyl-2-(5-oxovaleroyl) PC (POVPC) and 1-palmitoyl-2-glutaroyl PC (PGPC) associated with ischemia and reperfusion [80]. The pathophysiological mechanisms associated with myocardial damage after AMI remain unclear. Lipids are the primary targets of ROS, the levels of which rise during ISC and even more during IR (reviewed in [81]). A study has identified lipid peroxidation products in patients with AMI due to IR [78]. It should be noted that oxidised lipids are present in small amounts *in vivo* and are difficult to quantify [82].

In our study, we observed a significant decrease in the abundance of PL species during ISC and IR, in particular, 48 species with q < 0.001 (Supplementary Tables S3). Of these, all had a lower abundance in IR than in CT (17 species of PC, 5 PE, 8 PI and 1 PA). PC, but also PE, are the main components of cell membranes, and changes in structural phospholipids have been associated with changes in membrane properties. These include Ca^{2+} imbalance and changes in the permeability of the myocardial membrane [67,83], which can lead to cell death by destabilisation of the membrane. Phospholipid metabolism is affected during myocardial ischemia, and most studies reporting modulation of the PL profile attribute these changes to oxidised phospholipids [78,80] and their degradation by phospholipase A2 (PLA2) with the formation of bioactive eicosanoids and lysoPLs, which are important inflammatory mediators [72,73,84].

In our study, we observed that the levels of 16 alkyl acyl phospholipids (8 alkyl acyl PC, 8 alkyl acyl PE) were significantly altered during ISC and IR (Fig. 4, Supplementary Tables S3 and S4). These results show that, generally, the relative abundance of alkyl acyl phospholipids was lower in IR than in CT (11 species), lower in IR than in ISC (10 species) and lower in CT than in ISC (7 species). The MS/MS spectra did not allow the discrimination of plasmanyl and plasmenyl (plamalogen) species. As such, we did not assign them, except for (PE (P-38:6) and PE (P-40:7)), which were assigned as PE plasmalogens. However, since cardiac tissue contains high levels of plasmalogens, with a higher amount of plasmenyl ethanolamines (approximately 43–59% of PEs and approximately

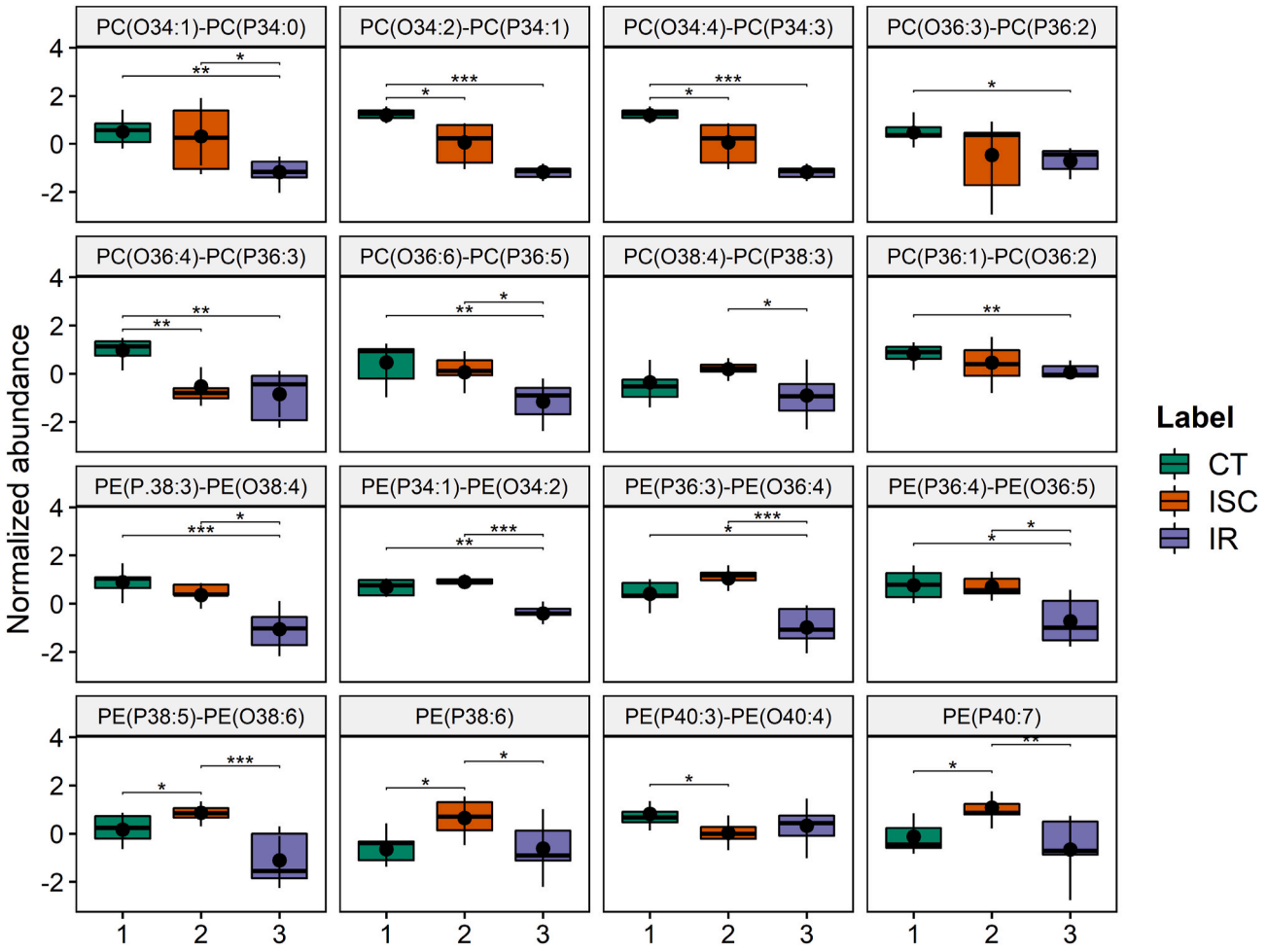

Fig. 4. Boxplots of significantly different alkyl acyl phospholipids species. Statistical tests were performed using the Kruskal-Wallis test followed by Dunn's multiple comparison test. Lipid species labels are in the following notation: PL (AC:N) (PL = phospholipid class; A = P (plasmenyl/plasmalogen) or O (plasmanyl); C = total of carbon atoms in fatty acids; N = number of double bonds). Three groups were studied: 1-Control (CT), 2-ischemia (ISC) and 3-ischemia-reperfusion (IR) ****$q < 0.001$, ***$q < 0.001$, **$q < 0.01$, *$q < 0.05$.

30–40% of PCs are plasmalogens) [85], we may assume that most of these species are plasmalogens. A previous study reported a decrease in the concentration of phosphatidylcholine and phosphatidylcholine plasmalogens in the plasma and serum of patients with incident myocardial infarction [31,86]. A decrease in circulating PE plasmalogens in the serum of patients with AMI has also been observed [31]. Consistently, other studies have implicated a decrease in plasmalogens in cardiovascular disease [29,31,75,76,87]. The results obtained in our study associated the variation of these plasmalogens also in cardiac tissue. Although plasmalogens are abundant in important functional organs, such as the heart, its role is far from fully understood, but it appears to play a crucial role in health and disease [88–90]. Among other functions, they have been reported to be crucial antioxidants during cellular oxidative stress, regarded as essential endogenous antioxidants and ROS scavengers [91,92]. Under oxidative stress, the plasmalogens are preferentially oxidised and avoid damage by lipid peroxidation, which may justify the reduction of the PE and PC plasmalogens in IR and ISC observed in our study. The vinyl-ether bond at the *sn*-1 position of these plasmalogens can readily react with ROS, thus supporting their antioxidant role [89]. Our study reinforces this argument, but further studies are needed to elucidate this mechanism and the possible diagnostic role of Pls. Although the changes we report here are not tissue specific, some are expected to be observable in plasma and could be used as complements in the timely, accurate diagnosis, prognosis, and management of acute myocardial infarction.

Although cardiomyocytes occupy most of the cardiac volume, one cannot exclude the vital contribution of endothelial cells, fibroblasts, and immune cells response ischemia/reperfusion injury. In addition, it is also conceivable that organelle-specific differences may also take place. Langendorff heart perfusion model is an ex vivo model that relies on the use of fluid perfusion that differs from blood in several aspects, namely composition, viscosity, and oxygenation capacity, which probably has an impact on the energetic and metabolic status ultimately affecting the phospholipidome. Thus, the analysis of the results observed between the control samples, the ischemic samples and the IR heart sample should be cautious because the changes observed after the reperfusion event are mainly affected by the reperfusion event and the ischemic event, but also by the nature of the ex vivo experience.

In summary, this study has demonstrated a clear change in the phospholipid profile during ischemia and reperfusion, with an overall decrease in the levels of some of the phospholipids, including PCs, PIs and PEs containing PUFAs and PE plasmalogens. We have also observed a decrease in some lysoPLs under these conditions. In general, the changes detected were more pronounced in IR than in ISC, which is consistent with the hypothesis that a large part of myocardial damage occurs during reperfusion. Our results provide molecular evidence for the impact of AMI on the lipidome of myocardial tissue and open new perspectives on the role of lipids in its pathophysiology, which could be useful for developing new therapeutic strategies and new diagnostic markers.

Author contributions

Tânia Melo, Tânia Martins-Marques, Henrique Girão, Rosario Domingues and Pedro Domingues contributed to the conceptualization; Javier Bullon, Susana Aveiro, Tânia Melo, Rosario Domingues and Pedro Domingues contributed to the methodology, investigation and data analysis, all authors contributed to writing—review and editing the manuscript.

Funding

This work was supported by funding from European Commission's Horizon 2020 research and innovation program under the Marie Sklodowska-Curie grant agreement number 675132 (MSCA-ITN-ETN MASSTRPLAN) to the University of Aveiro. Thanks are due to the University of Aveiro and FCT/MCT for the financial support to QOPNA ((FCT UID/QUI/00062/2019) and LAQV/REQUIMTE (UIDB/50006/2020), CESAM (UIDB/50017/2020 + UIDP/50017/2020) and to RNEM, Portuguese Mass Spectrometry Network, (LISBOA-01-0145-FEDER-402-022,125) through national funds and, where applicable, co-financed by the FEDER, within the PT2020 Partnership Agreement. This work was supported by the European Regional Development Fund (ERDF) through the Operational Program for Competitiveness Factors (COMPETE) [under the projects PAC "NETDIAMOND" POCI-01-0145-FEDER-016,385; HealthyAging2020 CENTRO-01-0145-FEDER-000012-N2323; POCI-01-0145-FEDER-007440, CENTRO-01-0145-FEDER-032,179, CENTRO-01-0145-FEDER-032,414 and FCTUID/NEU/04539/2013 to CNC. IBILI]. TMM was supported by PD/BD/106,043/2015 from Fundação para a Ciência e a Tecnologia (FCT).

Declaration of competing interest

The authors declare no conflict of interest.

Appendix A. Supplementary data

Supplementary data to this article can be found online at https://doi.org/10.1016/j.bbrep.2021.101037.

Pedro Domingues.

References

[1] S. Mendis, et al., World Health Organization definition of myocardial infarction: 2008-09 revision, Int. J. Epidemiol. 40 (2011) 139–146.
[2] M. Tibaut, D. Mekis, D. Petrovic, Pathophysiology of myocardial infarction and acute management strategies, Cardiovasc. Hematol. Agents Med. Chem. 14 (2017) 150–159.
[3] R.B. Jennings, Historical perspective on the pathology of myocardial ischemia/reperfusion injury, Circ. Res. 113 (2013) 428–438.
[4] D.J. Hausenloy, D.M. Yellon, The mitochondrial permeability transition pore: its fundamental role in mediating cell death during ischaemia and reperfusion, J. Mol. Cell. Cardiol. 35 (2003) 339–341.
[5] B. Soussi, J.-P. Idström, T. Schersten, A.-C. Bylund-Fellenius, Cytochrome c oxidase and cardiolipin alterations in response to skeletal muscle ischaemia and reperfusion, Acta Physiol. Scand. 138 (1990) 107–114.
[6] M. Neri, et al., Cardiac oxidative stress and inflammatory cytokines response after myocardial infarction, Curr. Vasc. Pharmacol. 13 (2015) 26–36.
[7] G.A. Kurian, R. Rajagopal, S. Vedantham, M. Rajesh, The role of oxidative stress in myocardial ischemia and reperfusion injury and remodeling: revisited, Oxid. Med. Cell. Longev. (2016) (2016) 1–14.
[8] S.-B. Ong, et al., Inflammation following acute myocardial infarction: multiple players, dynamic roles, and novel therapeutic opportunities, Pharmacol. Ther. 186 (2018) 73–87.
[9] R.S. Williams, I.J. Benjamin, Protective responses in the ischemic myocardium, J. Clin. Invest. 106 (2000) 813–818.
[10] T.K. Rudolph, et al., Nitro-fatty acids reduce atherosclerosis in apolipoprotein E-deficient mice, Arterioscler. Thromb. Vasc. Biol. 30 (2010) 938–945.
[11] Å.B. Gustafsson, R.A. Gottlieb, A.B. Gustafsson, R.A. Gottlieb, Autophagy in ischemic heart disease, Circ. Res. 104 (2009) 150–158.
[12] S. Ma, Y. Wang, Y. Chen, F. Cao, The role of the autophagy in myocardial ischemia/reperfusion injury ☆, Biochim. Biophys. Acta (BBA) - Mol. Basis Dis. 1852 (2015) 271–276.
[13] C. Huang, et al., Autophagy induced by ischemic preconditioning is essential for cardioprotection, J Cardiovasc. Transl. Res. 3 (2010) 365–373.
[14] T. Martins-Marques, et al., Ischaemia-induced autophagy leads to degradation of gap junction protein connexin 43 in cardiomyocytes, Biochem. J. 467 (2015) 231–245.
[15] G. Simonis, R.H. Strasser, B. Ebner, Reperfusion injury in acute myocardial infarction, Crit. Care 16 (2012) A22.
[16] S. Cadenas, ROS and redox signaling in myocardial ischemia-reperfusion injury and cardioprotection, Free Radic. Biol. Med. 117 (2018) 76–89.
[17] D.N. Granger, P.R. Kvietys, Reperfusion injury and reactive oxygen species: the evolution of a concept, Redox Biol 6 (2015) 524–551.
[18] K. Thygesen, et al., Third universal definition of myocardial infarction, Circulation 126 (2012).
[19] M.F.M. Fathil, et al., Diagnostics on acute myocardial infarction: cardiac troponin biomarkers, Biosens. Bioelectron. 70 (2015) 209–220.
[20] D.E. Farthing, C.A. Farthing, L. Xi, Inosine and hypoxanthine as novel biomarkers for cardiac ischemia: from bench to point-of-care, Exp. Biol. Med. 240 (2015) 821.
[21] L.H. Opie, Metabolic management of acute myocardial infarction comes to the fore and extends beyond control of hyperglycemia, Circulation 117 (2008) 2172–2177.
[22] L. Feng, et al., Lipid biomarkers in acute myocardial infarction before and after percutaneous coronary intervention by lipidomics analysis, Med. Sci. Mon. Int. Med. J. Exp. Clin. Res. 24 (2018) 4175–4182.
[23] N. Sawada, et al., Circulating oxidized LDL, increased in patients with acute myocardial infarction, is accompanied by heavily modified HDL, J. Lipid Res. 61 (2020) 816–829.
[24] Y. Sun, et al., Plasma fatty acids, oxylipins, and risk of myocardial infarction: the Singapore Chinese Health Study, J. Lipid Res. 57 (2016) 1300–1307.
[25] J.Y. Park, S.-H. Lee, M.-J. Shin, G.-S. Hwang, Alteration in metabolic signature and lipid metabolism in patients with angina pectoris and myocardial infarction, PloS One 10 (2015), e0135228.
[26] H. Hinterwirth, C. Stegemann, M. Mayr, Lipidomics: quest for molecular lipid biomarkers in cardiovascular disease, Circ. Cardiovasc. Genet. 7 (2014) 941–954.
[27] A. Ganna, et al., Large-scale metabolomic profiling identifies novel biomarkers for incident coronary heart disease, PLoS Genet. 10 (2014), e1004801.
[28] A. Sigruener, et al., Glycerophospholipid and sphingolipid species and mortality: the ludwigshafen risk and cardiovascular health (luric) study, PloS One 9 (2014), e85724.
[29] P.J. Meikle, et al., Plasma lipidomic analysis of stable and unstable coronary artery disease, Arterioscler. Thromb. Vasc. Biol. 31 (2011) 2723–2732.
[30] C. Syme, et al., Glycerophosphocholine metabolites and cardiovascular disease risk factors in adolescents: a cohort study, Circulation 134 (2016) 1629–1636.
[31] J.V. Moxon, et al., Baseline serum phosphatidylcholine plasmalogen concentrations are inversely associated with incident myocardial infarction in patients with mixed peripheral artery disease presentations, Atherosclerosis 263 (2017) 301–308.
[32] Y.K. Tham, et al., Distinct lipidomic profiles in models of physiological and pathological cardiac remodeling, and potential therapeutic strategies, Biochim. Biophys. Acta Mol. Cell Biol. Lipids 1863 (2018) 219–234.
[33] M. Nam, Y. Jung, D.H. Ryu, G.-S. Hwang, A metabolomics-driven approach reveals metabolic responses and mechanisms in the rat heart following myocardial infarction, Int. J. Cardiol. 227 (2017) 239–246.
[34] G. Paradies, et al., Decrease in mitochondrial complex I activity in ischemic/reperfused rat heart: involvement of reactive oxygen species and cardiolipin, Circ. Res. 94 (2004) 53–59.
[35] M.R. Reforgiato, et al., Inhibition of ceramide de novo synthesis as a postischemic strategy to reduce myocardial reperfusion injury, Basic Res. Cardiol. 111 (2016) 12.
[36] M. Knapp, et al., Myocardial infarction differentially alters sphingolipid levels in plasma, erythrocytes and platelets of the rat, Basic Res. Cardiol. 107 (2012) 294.
[37] M. Knapp, M. Zendzian-Piotrowska, K. Kurek, A. Blachnio-Zabielska, Myocardial infarction changes sphingolipid metabolism in the uninfarcted ventricular wall of the rat, Lipids 47 (2012) 847–853.
[38] A. Beresewicz, A. Dobrzyń, J. Górski, Accumulation of specific ceramides in ischemic/reperfused rat heart; effect of ischemic preconditioning, J. Physiol. Pharmacol. Off. J. Pol. Physiol. Soc. 53 (2002) 371–382.
[39] B. Sousa, et al., Alteration in phospholipidome profile of myoblast h9c2 cell line in a model of myocardium starvation and ischemia, J. Cell. Physiol. 231 (2016) 2266–2274.
[40] D.J. Herr, S.E. Aune, D.R. Menick, Induction and assessment of ischemia-reperfusion injury in Langendorff-perfused rat hearts, J. Vis. Exp. JoVE (2015), e52908, https://doi.org/10.3791/52908.
[41] V. Matyash, G. Liebisch, T.V. Kurzchalia, A. Shevchenko, D. Schwudke, Lipid extraction by methyl-tert-butyl ether for high-throughput lipidomics, J. Lipid Res. 49 (2008) 1137–1146.
[42] E.M. Bartlett, D.H. Lewis, Spectrophotometric determination of phosphate esters in the presence and absence of orthophosphate, Anal. Biochem. 36 (1970) 159–167.
[43] B. Sousa, et al., Alteration in phospholipidome profile of myoblast H9c2 cell line in a model of myocardium starvation and ischemia, J. Cell. Physiol. 231 (2016) 2266–2274.
[44] T. Pluskal, S. Castillo, A. Villar-Briones, M. Oresic, MZmine 2: modular framework for processing, visualizing, and analyzing mass spectrometry-based molecular profile data, BMC Bioinf. 11 (2010) 395.
[45] R Core Team. *R*, A Language and Environment for Statistical Computing, R Foundation for Statistical Computing, Vienna, Austria, 2018.
[46] Rstudio Team, Rstudio: Integrated Development Environment for R, 2016.

[47] Y.V. Karpievitch, S.B. Nikolic, R. Wilson, J.E. Sharman, L.M. Edwards, Metabolomics data normalization with Eigenms, PloS One 9 (2014), e116221.
[48] J. Xia, D.S. Wishart, Using Metaboanalyst 3.0 for comprehensive metabolomics data analysis, in: Current Protocols in Bioinformatics, 55 14, John Wiley & Sons, Inc., 2016, pp. 10.1–14.10.91.
[49] W. Stacklies, H. Redestig, M. Scholz, D. Walther, J. Selbig, pcaMethods a bioconductor package providing PCA methods for incomplete data, Bioinformatics 23 (2007) 1164–1167.
[50] Y. Benjamini, Y. Hochberg, Controlling the false discovery rate: a practical and powerful approach to multiple testing, WileyRoyal Statistical Society, J. Roy. Stat. Soc. B 57 (1995).
[51] H. Wickham, Ggplot2 – Elegant Graphics for Data Analysis, Springer Verlag, New York, 2016.
[52] H. Wickham, The split-apply-combine strategy for data analysis, J. Stat. Software 40 (2011).
[53] H. Wickham, R. François, L. Henry, K. dplyr Müller, A Grammar of Data Manipulation. R Package Version 0.7.7, 2018.
[54] H. Wickham, L. Henry, Tidyr: Easily Tidy Data with 'spread( )' and 'gather( )' Functions, 2018.
[55] K. Slowikowski, Ggrepel: Automatically Position Non-Overlapping Text Labels with 'ggplot2'. R Package Version 0.8.0, 2018.
[56] B. Cordeiro, R. Clements, Murine isolated heart model of myocardial stunning associated with cardioplegic arrest, J. Vis. Exp. JoVE (2015), e52433, https://doi.org/10.3791/52433.
[57] M. Klainguti, et al., Lack of nuclear apoptosis in cardiomyocytes and increased endothelin-1 levels in a rat heart model of myocardial stunning, Basic Res. Cardiol. 95 (2000) 308–315.
[58] G.C. Shearer, J. Chen, Y. Chen, W.S. Harris, Myocardial infarction does not affect fatty-acid profiles in rats, Prostaglandins Leukot. Essent. Fatty Acids 81 (2009) 411–416.
[59] A.I. Ostermann, M. Müller, I. Willenberg, N.H. Schebb, Determining the fatty acid composition in plasma and tissues as fatty acid methyl esters using gas chromatography – a comparison of different derivatization and extraction procedures, Prostaglandins Leukot. Essent. Fatty Acids 91 (2014) 235–241.
[60] E.D. Dodds, M.R. McCoy, L.D. Rea, J.M. Kennish, Gas chromatographic quantification of fatty acid methyl esters: flame ionization detection vs. Electron impact mass spectrometry, Lipids 40 (2005) 419–428.
[61] Z.H. Alshehry, et al., Plasma lipidomic profiles improve on traditional risk factors for the prediction of cardiovascular events in type 2 diabetes mellitus, Circulation 134 (2016) 1637–1650.
[62] S. Kohno, A.L. Keenan, J.M. Ntambi, M. Miyazaki, Lipidomic insight into cardiovascular diseases, Biochem. Biophys. Res. Commun. (2018).
[63] P. Wurtz, et al., Metabolite profiling and cardiovascular event risk: a prospective study of 3 population-based cohorts, Circulation 131 (2015) 774–785.
[64] C.D.L. Folmes, D. Sowah, A.S. Clanachan, G.D. Lopaschuk, High rates of residual fatty acid oxidation during mild ischemia decrease cardiac work and efficiency, J. Mol. Cell. Cardiol. 47 (2009) 142–148.
[65] J.-F. Llitjos, J.-P. Mira, J. Duranteau, A. Cariou, Hyperoxia toxicity after cardiac arrest: what is the evidence? Ann. Intensive Care 6 (2016) 23.
[66] F. Sjöberg, et al., The medical use of oxygen: a time for critical reappraisal, J. Intern. Med. 274 (2013) 505–528.
[67] V.K. Vishwakarma, P.K. Upadhyay, J.K. Gupta, H.N. Yadav, Pathophysiologic role of ischemia reperfusion injury: a review, J. Indian Coll. Cardiol. 7 (2017) 97–104.
[68] H. Budib Dorsa Pontes, et al., Ischemia and reperfusion injury: general aspects and mechanisms, EC Cardiology 2 (2016).
[69] S.T. Tan, T. Ramesh, X.R. Toh, L.N. Nguyen, Emerging roles of lysophospholipids in health and disease, Prog. Lipid Res. 80 (2020), 101068.
[70] T. Schönberger, et al., Pivotal role of phospholipase d1 in tumor necrosis factor-α–mediated inflammation and scar formation after myocardial ischemia and reperfusion in mice, Am. J. Pathol. 184 (2014) 2450–2464.
[71] M.-A. Urbahn, et al., Phospholipase D1 regulation of TNF-alpha protects against responses to LPS, Sci. Rep. 8 (2018), 10006.
[72] N.D. Hung, M.R. Kim, D.-E. Sok, Mechanisms for anti-inflammatory effects of 1-[15 (S)-hydroxyeicosapentaenoyl] lysophosphatidylcholine, administered intraperitoneally, in zymosan A-induced peritonitis, Br. J. Pharmacol. 162 (2011) 1119–1135.
[73] O.A. Akerele, S.K. Cheema, Fatty acyl composition of lysophosphatidylcholine is important in atherosclerosis, Med. Hypotheses 85 (2015) 754–760.
[74] A. Reis, C.M. Spickett, Chemistry of phospholipid oxidation, Biochim. Biophys. Acta Rev. Biomembr. 1818 (2012) 2374–2387.
[75] I. Sutter, et al., Decreased phosphatidylcholine plasmalogens – a putative novel lipid signature in patients with stable coronary artery disease and acute myocardial infarction, Atherosclerosis 246 (2016) 130–140.
[76] I. Sutter, et al., Plasmalogens of high-density lipoproteins (HDL) are associated with coronary artery disease and anti-apoptotic activity of HDL, Atherosclerosis 241 (2015) 539–546.
[77] W. Li, et al., Profile of cardiac lipid metabolism in STZ-induced diabetic mice, Lipids Health Dis. 17 (2018) 231.
[78] J. Lu, et al., Comprehensive metabolomics identified lipid peroxidation as a prominent feature in human plasma of patients with coronary heart diseases, Redox Biol 12 (2017) 899–907.
[79] C. Yeang, et al., Reduction of myocardial ischaemia–reperfusion injury by inactivating oxidized phospholipids, Cardiovasc. Res. 115 (2019) 179–189.
[80] R. Ganguly, et al., Alpha linolenic acid decreases apoptosis and oxidized phospholipids in cardiomyocytes during ischemia/reperfusion, Mol. Cell. Biochem. 437 (2018) 163–175.
[81] T. Zhou, E.R. Prather, D.E. Garrison, L. Zuo, Interplay between ROS and antioxidants during ischemia-reperfusion injuries in cardiac and skeletal muscle, Int. J. Mol. Sci. 19 (2018).
[82] Y.Y. Tyurina, et al., Redox lipidomics technology: looking for a needle in a haystack, Chem. Phys. Lipids 221 (2019) 93–107.
[83] H. Budib Dorsa Pontes, et al., Ischemia and reperfusion injury: general aspects and mechanisms, EC Cardiology 2 (2016).
[84] F.A. Fitzpatrick, R. Soberman, Regulated formation of eicosanoids, J. Clin. Invest. 107 (2001) 1347–1351.
[85] N. Nagan, R.A. Zoeller, Plasmalogens: biosynthesis and functions, Prog. Lipid Res. 40 (2001) 199–229.
[86] Ž. Reiner, et al., Lipid lowering drug therapy in patients with coronary heart disease from 24 European countries – findings from the EUROASPIRE IV survey, Atherosclerosis 246 (2016) 243–250.
[87] M. Nishimukai, et al., Serum choline plasmalogens—those with oleic acid in sn–2—are biomarkers for coronary artery disease, Clin. Chim. Acta 437 (2014) 147–154.
[88] J.M. Dean, I.J. Lodhi, Structural and functional roles of ether lipids, Protein Cell 9 (2018) 196–206.
[89] J. Lessig, B. Fuchs, Plasmalogens in biological systems: their role in oxidative processes in biological membranes, their contribution to pathological processes and aging and plasmalogen analysis, Curr. Med. Chem. 16 (2009) 2021–2041.
[90] S. Paul, G.I. Lancaster, P.J. Meikle, Plasmalogens: a potential therapeutic target for neurodegenerative and cardiometabolic disease, Prog. Lipid Res. 74 (2019) 186–195.
[91] S. Wallner, Plasmalogens the neglected regulatory and scavenging lipid species, Chem. Phys. Lipids 164 (2011) 573–589.
[92] M. Hermansson, K. Hokynar, P. Somerharju, Mechanisms of glycerophospholipid homeostasis in mammalian cells, Prog. Lipid Res. 50 (2011) 240–257.